SLAC–PUB–95–6523

A Technique of Measuring and Correcting Emittance Dilutions due to Accelerator Structure Misalignments*

T. O. Raubenheimer and K. Kubo*

Stanford Linear Accelerator Center
Stanford University, Stanford, California 94309

ABSTRACT

This paper describes a method of reducing the transverse emittance dilution in linear colliders due to transverse wakefields arising from misaligned accelerator structures. The technique is a generalization of the Wake-Free [5] correction algorithm. The structure errors are measured locally by varying the bunch charge and/or bunch length and measuring the change in the beam trajectory. The structure errors can then be corrected by varying the trajectory or moving the structures. The results of simulations are presented demonstrating the viability of the technique.

Submitted to *Nuclear Instruments and Methods*

★ Work supported by Department of Energy contract DE–AC03–76SF00515.
★ Permanent address: KEK, 1–1 Oho, Tsukuba, Ibaraki-ken 305, Japan

1. Introduction

A number of e^+e^- linear colliders are being designed with center-of-mass energies from 0.5 to 1.5 TeV. One of the major problems facing these designs is the preservation of the transverse emittance through the multi-kilometer linear accelerators [1]. In the linacs, the magnets, accelerating structures, and beam position monitors (BPMs) are all misaligned with respect to the ideal centerline and thus the beam is offset in the magnets and the structures. This can lead to both dispersive errors and transverse wakefields which dilute the projected transverse emittance and thereby reduce the collider's luminosity. In this paper, we will discuss a new approach to aligning the accelerator structures.

In most designs, the magnets and structures must be aligned with an accuracy on the order of microns [2]. This alignment would be extremely difficult to achieve and maintain with a mechanical alignment system [3] and thus a number of beam-based alignment procedures have been proposed to align the BPMs and the quadrupole magnets [4–8]. These beam-based procedures utilize information from the response of the beam to changes in the strength of the quadrupole magnets; the resulting alignment accuracy depends upon the BPM resolution (reading-to-reading measurement jitter) and is insensitive to the initial alignment [9].

Unfortunately, these techniques cannot be used to align the accelerating structures. At this time, there are four approaches to the structure alignment: (1) extremely accurate mechanical alignment; (2) direct measurement of the dipole mode (transverse wakefield) excited by the beam in the structure; (3) alignment by mechanically attaching a very accurate BPM to the structure; and (4) trajectory bumps, tuned by emittance measurements, which correct the effect of the emittance dilutions. Although all of these techniques will work at some level, it may be difficult to achieve the required accuracy and emittance preservation. In this paper, we present an alternate method, first suggested in ref. [5], which is similar to the beam-based alignment techniques for the quadrupoles. Although this technique will also be difficult to implement, it is an alternate approach that is worthy of consideration.

Finally, we should note that there are two approaches to the correction of the emittance dilutions in a linear accelerator: "local" correction and "global" correction [1]. Because the wakefield dilutions are conservative dilutions, we do not need to correct the structure errors locally; indeed, we only need to correct the errors before the beam filaments (phase mixes). Thus, to correct an error at some point in the linac, we can apply a correction a long distance away, separated by $n\pi$ in betatron phase, based upon direct measurements of the beam emittance. The first three solutions to the cavity alignment problem are local corrections, while the fourth solution is a global correction technique.

A problem with the global correction is that the correction is less stable than if the sources of dilution were corrected locally. One large effect, namely the dilution, is canceled with another, namely the correction, and thus the resulting emittance is very sensitive to the stability of the betatron phase advance. The phase advance sensitivity changes continuously as the klystron population and magnets fluctuate. Thus, it is advantageous to perform the correction locally; this is the emphasis in our paper. In the next sections, we outline our technique and then present the results of simulations demonstrating the viability of the approach.

2. Theory

Transverse wakefields result from the electro-magnetic interaction between the particle bunch and its surroundings, namely, the acceleration structures. When a point charge travels off-axis in a structure, it leaves behind a transverse wakefield that will deflect subsequent particles. Thus, when a beam travels off-axis through an accelerating structure, the transverse wakefield deflects the tail of the beam. This has two effects: it increases the projected emittance of the beam, and it deflects the beam centroid. The centroid deflections can be used to determine the offsets of the structures relative to the beam.

In most designs, the magnitude of the deflections is very small, and thus one cannot detect the deflections directly; the wakefield deflections are masked by kicks from the quadrupoles and the absolute BPM alignment errors. Instead, to measure the structure misalignments, we vary the wakefield kicks induced by the structures and then measure the resulting change in the trajectory. This measurement is then limited by the BPM resolution, the reading-to-reading measurement jitter, which is usually much smaller than the absolute alignment error. Furthermore, because numerous BPMs are located through the linac, this measurement provides local information about the structure misalignments.

Finally, we correct for the structure alignment errors by either steering the trajectory or moving the structures. If we correct for the structure misalignments by steering the trajectory, we must be careful not to generate dispersive errors. This could be avoided by using non-dispersive bumps [10] or by combining the steering with dispersive error correction. Directly moving the structure also avoids this problem; this was noted in ref [11] in which the author proposed a global emittance correction scheme. As mentioned, we would like to perform the corrections in a local or quasi-local manner to improve the stability of the correction.

In this section, we will present the equations of motion and describe the effect of BNS damping and autophasing on the correction technique. We will then estimate the magnitude of the deflections and emittance dilutions, and, finally, we will describe the data measurement and analysis, and the implementation of the correction procedures.

2.1 Equations of Motion and Autophasing

The transverse equation of motion for a particle in a high-energy linear accelerator can be written [12]

$$\begin{aligned}\frac{1}{\gamma(s)}\frac{d}{ds}\gamma(s)\frac{d}{ds}x(s;z,\delta)+(1-\delta)K[x(s;z,\delta)-x_q]&=(1-\delta)G\\-\frac{(1-\delta)}{\gamma_0(s)}Nr_0\int_z^{\infty}dz'\int_{-\infty}^{\infty}d\delta'\rho(z',\delta')W_{\perp}(s;z-z')[x(s;z',\delta')-x_a]&\quad,\end{aligned}\tag{2.1}$$

where s and z are the longitudinal position in the accelerator and in the bunch, respectively and δ is the relative energy deviation: $\delta=\big(\gamma(s)-\gamma_0(s)\big)/\gamma(s)\ll 1$; note that the energy deviation is also a function of s and z. Next, K and G are the normalized focusing and bending functions: $K(s)=\frac{e}{p_0c}\frac{dB_y}{dx}$ and $G(s)=\frac{e}{p_0c}B_y$, where p_0 is the design particle momentum and B_y is the vertical component of the magnetic field. Finally, N and r_0 are the number of particles and the classical electron radius, $W_{\perp}$ and ρ are the transverse wakefield and the longitudinal distribution function for the particle bunch, and x_q and x_a are the misalignments of the quadrupoles and the accelerator structures.

Now, we can assume that the energy deviation and transverse wakefield are small and make a perturbative expansion similar to that ref. [13]: $x(z)=x_0+x_1(z)+\cdots$. Further assuming that the acceleration gradient is small, so that the distance required to double the beam energy is small compared to the betatron wavelength, the equations for the first three terms in the expansion are:

$$\begin{aligned}x_0''+Kx_0&=G+Kx_q\\x_1''(z)+Kx_1(z)&=-\delta(z)(G+Kx_q)+\delta(z)Kx_0-\big(1-\delta(z)\big)\frac{Nr_0}{\gamma_0}\mathcal{W}_1(z)\left[x_0-x_a\right]\\x_2''(z)+Kx_2(z)&=\delta(z)Kx_1(z)-\big(1-\delta(z)\big)\frac{Nr_0}{\gamma_0}\int_z^{\infty}dz'\rho(z')W_{\perp}(z-z')x_1(z')\quad,\end{aligned}\tag{2.2}$$

where the wakefield integral in the equation for x_1 has been expressed as the function $\mathcal{W}_1$:

$$\mathcal{W}_1(z)\equiv\int_z^{\infty}dz'\rho(z')W_{\perp}(z-z')\quad,\tag{2.3}$$

since x_0 and x_a do not depend upon z. In the case of a gaussian bunch and a linear wakefield $W_{\perp}(z)=W'z$, which is an excellent approximation for the short-range wakefield of a periodic structure, $\mathcal{W}_1$ can be evaluated as

$$\mathcal{W}_1(z) = \frac{W'}{2}\left[z - \operatorname{erf}\left(\frac{z}{\sqrt{2}\sigma_z}\right)z - 2\frac{\sigma_z e^{-z^2/2\sigma_z^2}}{\sqrt{2\pi}}\right] \quad . \tag{2.4}$$

The solutions of eq. (2.2) are easily found in terms of the initial values and an integration of the driving terms over the Greens function for the focusing structure of the linac:

$$\begin{aligned}
x_0(s) &= x_0(s_0)R_{11}(s,s_0) + x_0'(s_0)R_{12}(s,s_0) + \int_{s_0}^{s} ds'(G + Kx_q)R_{12}(s,s') \\
x_1(s,z) &= \int_{s_0}^{s} ds'\big[\delta(G + Kx_q) + \delta K x_0 - (1-\delta)\frac{Nr_0}{\gamma_0}\mathcal{W}_1(x_0 - x_a)\big]R_{12}(s,s') \\
x_2(s,z) &= \int_{s_0}^{s} ds'\big[\delta K x_1 - (1-\delta)\frac{Nr_0}{\gamma_0}\int_{z}^{\infty} dz'\rho W_\perp x_1\big]R_{12}(s,s') \quad .
\end{aligned} \tag{2.5}$$

Here, R_{11} and R_{12} are elements of the linear transport matrix for the focusing structure of the linac; the $R_{11}(s,s_0)$ term relates the position at s to the position at s_0, and the $R_{12}(s,s_0)$ term relates the position at s to the angle at s_0.

At this point, we need to describe the autophasing techniques [14–16] that are utilized in all of the linear collider designs. Autophasing attempts to cancel the effect of the wakefield by varying the beam energy or the focusing along the bunch. Specifically, a correlated energy deviation $\delta(z)$ or a variation in the quadrupole strength $\Delta K(z)$ is chosen so that the term $\big[\delta(z)K - \big(1-\delta(z)\big)\frac{Nr_0}{\gamma_0}\mathcal{W}_1(z)\big]x_0$ approximately cancels. The energy deviation can be induced by running off the crest of the rf accelerating voltage or the variation in quadrupole focusing can be created using RFQs.

In the smooth approximation, where K and $\mathcal{W}_1$ are smooth functions of s, one can solve for a $\delta(z)$ such that this term $[\delta K - (1-\delta)\frac{Nr_0}{\gamma_0}\mathcal{W}_1(z)]$ is always zero. This will cancel all wakefield effects arising from a betatron oscillation and the beam will oscillate coherently. Unfortunately, this local cancellation is not possible [17] in the alternating gradient focusing structures used in high-energy machines. While the wakefield $W_\perp$ has a constant sign, an alternating-gradient focusing structure usually contains a periodic array of discrete focusing magnets with both positive and negative K values. Since the energy deviation $\delta(z)$ cannot be changed rapidly with s, at best one can adjust $\delta(z)$ to cancel the integral of this term. Furthermore, since this cancellation depends upon the position x_0 in the quadrupoles and the accelerator sections, exact cancellation is only possible if $x_0(s)$ is correlated from point to point. This is the case for a coherent betatron oscillation, but it is not true if the particle is steered or deflected by random errors as is the case for a corrected trajectory or accelerator structure misalignments. Thus, while the autophasing technique can cancel the wakefield effects due to a betatron oscillation, in first order, it has no effect on the dilutions arising from wakefields due to a corrected trajectory or those due to structure misalignments.

Regardless, autophasing is very important because it prevents the wakefield dilutions due to the misaligned structures from growing. In fact, with the autophasing energy spread, the dilutions are actually damped. To see this, we need to look at the second-order solution. Assuming the autophasing condition, the second-order solution can be written:

$$x_2(z) \propto (1-\delta)\mathcal{W}_1(z)x_1(z) - (1-\delta)\int_z^{\infty} dz'\rho(z')W_\perp(z-z')x_1(z') \quad , \tag{2.6}$$

where we have neglected the integrals over s and the R_{12}. Further assuming that $x_1(z)$ is due to a misaligned accelerator structure, then $x_1(z) \propto \mathcal{W}_1(z)x_a$ and the second order solution is

$$x_2(z) \propto x_a(1-\delta)\left[\mathcal{W}_1(z)^2 - \int_z^{\infty} dz'\rho(z')W_\perp(z-z')\mathcal{W}_1(z')\right] \quad , \tag{2.7}$$

where the integral over $W_\perp$ and $\mathcal{W}_1$ can be defined as $\mathcal{W}_2(z)$ in the same manner as eq. (2.3). In most cases, $\mathcal{W}_1^2 \gg \mathcal{W}_2$; for example, assuming a gaussian bunch and a linearly increasing wakefield, $\mathcal{W}_1^2(z)$ is roughly six times larger than $\mathcal{W}_2(z)$. Thus, an autophasing-like cancellation does not occur. Instead, the wakefield deflections are actually damped, much like the centroid oscillations are damped in the BNS damping regime [14, 18].

This damping of the deflections due to misaligned structures is illustrated in fig. 1 where we have plotted the normalized amplitude of the beam centroid:

$$\gamma J \equiv \frac{\gamma}{2}\left[\frac{1+\alpha^2}{\beta}\langle y\rangle^2 + 2\alpha\langle y\rangle\langle y'\rangle + \beta\langle y'\rangle^2\right] \quad , \tag{2.8}$$

for two cases in the first two-thirds of the SLAC 500–GeV center of mass NLC design [19]; parameters are listed in table 1. In the first case (solid), the beam is initially offset by $0.1\sigma_y$ and oscillates down the linac. In the second case (dashes), one structure at the beginning of the linac is offset by $100\,\mu$m. The offset structure deflects the tail of the beam, causing the beam centroid to oscillate. In both cases, the centroid oscillates by roughly 10% of the beam size, but, in the first case, the oscillation does not damp rapidly because the beam is close to the autophasing condition. In contrast, the oscillation due to the wakefield deflection is damped rapidly by the wakefields. In both cases, the oscillation damps rapidly at the end of the linac due to filamentation of the beam tails.

2.2 Centroid Deflections and Emittance Dilution

Now, we can estimate the magnitude of the centroid deflections due to structure misalignments. Because the BNS damping will prevent growth of the induced oscillation, we will only consider the first-order contribution. Using eq. (2.5), the deflection of the bunch centroid is given by:

$$\begin{aligned} \theta_a &= x_a L_a \int_{-\infty}^{\infty} dz \rho(z) \frac{N r_0}{\gamma_0} \mathcal{W}_1(z) \\ &= x_a \frac{N r_0}{\gamma_0} \overline{\mathcal{W}}_1 L_a \quad , \end{aligned} \tag{2.9}$$

where, L_a is the length of the accelerating structure. For a gaussian beam and linear wakefields, this is equal to

$$\overline{\mathcal{W}}_1 = -\frac{\sigma_z W'}{\sqrt{\pi}} \quad . \tag{2.10}$$

As mentioned, the deflections are typically small. For example, in the SLAC 500–GeV center of mass NLC design, a 25–μm misalignment of a single 1.8–m structure at the beginning of the linac, where the beam energy is 10 GeV, will lead to a 0.15–μm oscillation. This is extremely small, roughly 15% of the BPM resolution. For comparison, a 25–μm misalignment of a quadrupole at the low energy end of the linac would lead to a 100–μm oscillation.

Of course, a single misaligned structure does not generate significant emittance dilution. We can use the first-order approximation to estimate the emittance dilution that would arise from the structure misalignments. For small dilutions, the first-order contribution to the emittance dilution is

$$\Delta\epsilon \approx \frac{\beta}{2} \int_{-\infty}^{\infty} dz \rho(z) \left[\left(x_a L_a \frac{N r_0}{\gamma_0} \mathcal{W}_1(z) \right)^2 - \theta_a^2 \right] \quad , \tag{2.11}$$

which, for a gaussian bunch and linear wakefields, is approximately

$$\Delta\epsilon \approx 0.91 \frac{\beta}{2} \theta_a^2 \quad , \tag{2.12}$$

where θ_a is given by eq. (2.10). Thus, we would expect less than 0.1% dilution from the previous example.

Although the effect of a single structure is small, there are thousands of structures in each linac, and the emittance dilution and the centroid deflection can become significant. Equation (2.10) is useful in that it relates the emittance dilution to the deflection of the beam centroid. For example, if we want to keep the emittance dilution to less than 6%, eq. (2.12) suggests that we need to limit the centroid deflections due to the wakefields to the level of $\sigma/4$; in the SLAC NLC design, this is roughly 0.5 μm.

2.3 Measurement

Because the wakefield deflections are so small, their effect on the trajectory will be masked by the misalignments of the BPMs and deflections due to the misaligned quadrupoles and the dipole correctors. Thus, to measure the wakefield deflections, we measure the *change* in trajectory while changing the bunch length or the bunch population. Of course, this difference trajectory is still very small, but, we can magnify the effects by comparing the trajectories of a short low-current bunch with that of a bunch having a charge and/or length much larger than nominal.

Ideally, we would like to make these changes without varying any other parameters of the bunch or the machine. Unfortunately, the beam energy and energy spread and the autophasing condition all change when either the bunch charge or the bunch length are varied. This has two principal effects: first, when the beam energy varies, dispersive errors will cause centroid fluctuations that would mask the effect of the wakefields. Second, if the autophasing condition and BNS damping are lost, the beam will become more sensitive to jitter, making it difficult to measure the change in trajectory due to the wakefields.

It might be possible to vary the bunch parameters along with the RF voltage and phase in some complicated manner, thereby preserving the beam energy and the autophasing condition, but this would add to the operational complexity of the measurements. The solution we adopted was to simply leave the linac parameters fixed, allowing the beam energy and energy spread to vary, and to correct the dispersive errors either during or prior to the correction.

This still leaves the problem of the autophasing condition and the jitter sensitivity. Fortunately, assuming that most of the energy spread for autophasing is generated by the longitudinal wakefield and not the slope of accelerating rf, the jitter sensitivity is roughly independent of the beam current. For example, in the SLAC NLC design, where the beam is accelerated 6° ahead of the rf crest, the jitter sensitivity doubles when the beam charge is decreased by 80% and decreases by a factor of two when the beam charge is doubled; this occurs because the energy spread induced by the longitudinal wakefield increases when the bunch charge increases. These remaining changes in jitter sensitivity could easily be compensated by decreasing the bunch length at lower currents and increasing the bunch length for higher current beams.

Finally, we should note that the BPM resolution is typically a function of the beam charge. Usually, it is possible to calibrate the BPMs for different beam charges, but this may not be possible during a measurement sequence; the calibration would likely add unacceptable systematic errors.

2.4 Correction Algorithm

As described, to solve for the structure misalignments, we measure a number of trajectories while varying various beam parameters such as the charge and the bunch length between measurements. In the first-order approximation of eq. (2.5), these measurements can be related to the structure offsets:

$$\vec{m} = \vec{m}_0 + \vec{\xi} + \mathbf{A}(N, \sigma_z)\vec{x}_a \quad . \tag{2.13}$$

Here, $\vec{m}_0$ is the static BPM reading offset arising from the BPM misalignment and the non-zero trajectory due to effects other than wakefields. In addition, $\vec{\xi}$ is a stochastic vector representing the reading-to-reading jitter on the BPM measurement and $\mathbf{A}$ is the linear matrix relating a structure offset to a position offset further down the linac.

To then make optimal use of this data, we utilize the Gauss-Markov theorem. This states that, given data with a covariance matrix $\mathbf{V}$:

$$V_{ij} = \langle x_{ai} x_{aj} \rangle - \langle x_{ai} \rangle \langle x_{aj} \rangle \quad , \tag{2.14}$$

and an unbiased matrix $\mathbf{A}$ relating the variables to the data, the minimum error in the solution is found from:

$$\overline{x_a} = \left(\widetilde{\mathbf{A}}\mathbf{V}^{-1}\mathbf{A}\right)^{-1} \widetilde{\mathbf{A}}\mathbf{V}^{-1}\vec{m} \quad . \tag{2.15}$$

In practice, we do not solve for the individual structure misalignments. Instead, we solve for either a new trajectory that will minimize the effect of the structure misalignments or we solve for the offsets of a reduced set of structures that will cancel the effect of the other misalignments. When solving for a new trajectory, we assume that the measurement errors arise from the BPM alignment errors and the finite BPM resolution (reading-to-reading jitter). In this case, the minimum-error solution is found by minimizing:

$$\chi_d^2 = \sum_{i\in BPM} \sum_{j}^{trajectories} \left[\frac{(m_{i,j} + x_{i,j})^2}{\sigma_{BPM}^2 + \sigma_{res}^2} + \sum_{k=1}^{j-1} \frac{(\Delta m_{i,j,k} + \Delta x_{i,j,k})^2}{\sigma_{res}^2} \right] \quad , \tag{2.16}$$

where $m_{i,j}$ is the measured position of the jth trajectory at the ith BPM, $x_{i,j}$ is the calculated position of the jth trajectory at the ith BPM as a function of the dipole correctors, $\Delta m_{i,j,k}$ is the measured difference between the jth and kth trajectories at the ith BPM, and $\Delta x_{i,j,k}$ is the calculated difference between the jth and kth trajectories at the ith BPM, again as a function of the dipole correctors. Finally, σ_{BPM} is the estimated misalignment of the BPMs and σ_{res} is the BPM resolution, the reading-to-reading jitter in the BPM measurement.

Alternately, when optimizing the position of a small set of structures, we are only concerned with minimizing the difference between trajectories with different bunch lengths and/or charges. In this case, we assume that the only error is due to the BPM resolution and thus we minimize:

$$\chi_m^2 = \sum_{i\in BPM} \sum_{j}^{trajectories} \sum_{k=1}^{j-1} \left[\frac{(\Delta m_{i,j,k} + \Delta x_{i,j,k})^2}{\sigma_{res}^2} \right] \quad . \tag{2.17}$$

In both cases, we can estimate the matrix **A**, which relates either the dipole correctors or the structure offsets to the trajectories analytically, or we can measure the matrix directly. When the wakefields are relatively weak, **A** is straightforward to estimate theoretically, but when the wakefields are more important, the linear calculations are no longer valid; the wakefields add significant non-linearity to the beam transport and we suggest using measurements to construct **A**.

3. Simulations

Tracking simulations were performed to test the correction technique on the SLAC 500-GeV center of mass NLC linac [19]; parameters of the linac are listed in Table 1. The simulation program [20] was written to track both single bunches and multi-bunch trains but in this study we only considered emittance dilutions of a single bunch. In the simulations, the bunch was divided longitudinally into ten slices and each slice was further subdivided into five macro particles with different initial energies; thus, the longitudinal phase space was represented with 50 macro particles. The initial distribution of the bunch length and the energy spread were assumed to be gaussian with a maximum extent of $\pm 2\sigma_z$. The rf accelerating field was assumed to be sinusoidal and the rf phase was determined to optimize the autophasing condition. The tracking included both the longitudinal and the transverse wakefields for the NLC structure. [21]

Although the bunch charge and bunch length are varied in the simulations, the amplitude and phase of the accelerating voltage and the magnetic fields of the quadrupole magnets and dipole correctors were kept constant. Thus, the beam energy and energy spread would vary because of the sinusoidal rf and the longitudinal wakefields and the transverse focusing would vary because of the variation in beam energy. Although this is not optimal for the correction procedure, it should make the operational implementation simpler. Finally, we should note that we have ignored any dependence of the BPM resolution on the beam charge in the simulations.

3.1 Correction of Misaligned Structures

At first, to separate the wakefield effects from the dispersive effects, only accelerating structures were misaligned; the quadrupoles and BPMs were aligned perfectly. For these simulations, the accelerating structures were misaligned with errors having a gaussian distribution with $\sigma = 50\,\mu\text{m}$ and truncated at $\pm 3\sigma$, and the BPMs were assumed to have a resolution (reading-to-reading jitter) of $\sigma_{res} = 1\,\mu\text{m}$.

As mentioned, we considered two methods of correction:

(*a*) Adjust the beam trajectory using dipole correctors,

(*b*) Move some of the accelerating structures.

In method (*a*), four trajectories with different bunch charge, bunch length, and quadrupole strengths were measured by BPMs located at the quads; the parameter values utilized are listed in table 2a. The strength of the dipole correctors, located at the quadrupoles, were then set to minimize χ^2_d, defined as eq. (2.16). In the simulations, we used theoretical values for the transport matrices, and because the transfer matrix with the energy spread and wakefields is not known exactly, the measurements and the fitting were iterated twice. For the fitting, the linac was divided into eight sections and the fitting was performed for each section where the adjacent sections overlapped slightly. In this case, the relative emittance growth was estimated as 13.6% from 100 different seeds. For comparison, before correcting the structures, the relative emittance growth was 170%, as found from 100 different distributions of errors.

In method (*b*), we moved accelerating structures instead of steering the trajectory. One structure every three FODO cells, or every six quads, was moved to minimize the χ^2_m, [eq. (2.17)]. The number of moving structures was 103 out of a total of 3622 structures. Three different trajectories with different bunch charges and lengths, as listed in table 2b, were measured by BPMs located at the quadrupoles and the moving structures; other parameters were the same as for case (a). Here, we found an average relative emittance growth of 8.1% from 100 different distributions of random errors; the simulation results are summarized in table 3.

Finally, we studied the effectiveness of the technique versus the strength of the wakefield. The effective strength of the transverse wakefield can be characterized by the centroid deflection eq. (2.10): $\Delta x/x_a = \beta L_a \frac{N r_0}{\gamma_0} \overline{W}_1(z)$. Thus, the effective strength of the wakefield depends on the magnitude of the wakefield, which is a function of the rf frequency and the aperture in the accelerating structures, the bunch length and charge, the beam energy, and the transverse focusing. When the effective strength of the wakefield is larger, the deflections are more easily measured and we can make smaller changes of the charge and/or bunch length. Figure 2 is a plot of the emittance dilution versus the slope of transverse wake field $W'_\perp$ in the SLAC NLC linac for three cases: no correction (solid), corrections changing both charge and length (dashes), and corrections changing only charge (dots); for reference, the NLC wakefield strength is $W'_\perp = 7 \times 10^{19}\,\mathrm{V/C/m^3}$. The apparent kink at $W' = 20 \times 10^{19}$ occurs because we re-optimized the rf phase for autophasing, changing it from $-6°$ to $-4°$. In all cases, the results were averaged from 100 different sets of random structure misalignments with $\sigma = 50\,\mu\mathrm{m}$ and the BPM $\sigma_{res} = 1\,\mu\mathrm{m}$. Finally, in the strong wakefield cases, we needed to divide the linac into 18 sections and iterate the fitting twice because the wakefields seriously perturb the beam transport—alternately, one could measure the correction matrix elements directly, thereby improving the convergence. Notice that the correction is roughly independent of the wakefield strength and can be very effective for designs with strong wakefields.

3.2 Correction of Misaligned Structures, Quadrupoles, and BPMs

At this point, we included alignment errors of the BPMs and quadrupoles, as well as alignment errors of the structures, in the correction simulations. Again, two methods were studied:

(*c*) Adjust the dipole correctors as in method (*a*), described in Section 3.1, to minimize both wakefield and dispersive effects simultaneously.

(*d*) First adjust the dipole correctors to minimize dispersive effect using low-current beams (DF correction [6]). Then, move the accelerating structures to minimize the wakefield effects as in method (*b*) described in Section 3.1.

In the simulation for method (*c*), five trajectories were measured and the dipole correctors were set to minimize χ_d^2, defined by eq. (2.16), in the same manner as method (*a*). The accelerating structures, quadrupole magnets, and BPMs were all independently misaligned with $\sigma = 50\,\mu\mathrm{m}$ (truncated $\pm 3\sigma$) and the resolution of the BPMs was $\sigma_{res} = 1.0\,\mu$m. The linac was divided into eight sections and the fitting was iterated four times for each section. The relative emittance growth was estimated as 14.4% from the average of 100 different sets of random errors; for comparison, the emittance growth was 1660% after using one-to-one trajectory correction.

In method (*d*), we first corrected the dispersive errors and then corrected the wakefield effects. In the first step, the bunch charge was set to be 0.1 of nominal charge and DF trajectory correction [6] was used to minimize the dispersive errors, i.e., three trajectories (see table 2d) were measured and the dipole correctors were set to minimize χ_d^2 as defined by eq. (2.16). In the second step, we corrected for wakefield effect using the same procedure as method (*b*). Three trajectories were measured and the accelerating structures were moved to minimize the difference between the trajectories, i.e., we minimized χ_m^2 [defined by eq. (2.17)]. We used two iterations in the first step and one iteration in the second step. All other parameters were the same as for method (*c*). In this case, the relative emittance growth was estimated as 20% from the average of 100 different sets of random errors. The simulation results for the SLAC 500-GeV NLC design are summarized in table 3 where we have assumed a BPM resolution of $\sigma_{res} = 1\,\mu$m.

Finally, fig. 3 illustrates the effectiveness of the correction technique versus the BPM resolution and the magnitude of the misalignments for four cases: 1-to-1 correction only (solid), method (d) with $\sigma_{res} = 2.0\,\mu$m (dashes), method (d) with $\sigma_{res} = 1.0\,\mu$m (dots), and method (d) with $\sigma_{res} = 0.5\,\mu$m (dash-dot); the simulations with $\geq 100\,\mu$m misalignments were performed using three times as many moving structures as nominal, i.e., 309 out of 3622. With 50-μm errors and one-to-one correction, the emittance dilution is over 1600%, while the wakefield correction techniques reduce the dilution to roughly 20%, assuming $\sigma_{res} = 1\,\mu$m. Notice that the wakefield correction is roughly independent of the magnitude of the misalignments, but depends upon the BPM resolution.

4. Discussion

In this paper, we have described a new technique for correcting the effects of misaligned accelerator structures. This is a beam-based technique where the effectiveness primarily depends upon the BPM resolution (reading-to-reading jitter) and not the initial structure alignment. It is a straightforward extension of the DF [6] and WF [5] techniques, which can be used to align the quadrupole magnets, to the problem of aligning the accelerating structures. Instead of studying the response of the beam to variations in the quadrupole strengths, to study the structure alignment, we suggest measuring the trajectory as a function of variations in the bunch length and/or intensity.

We have discussed the effect of the structure misalignments on the beam when considering both the wakefields and the energy spread required for autophasing. In the autophasing regime, betatron oscillations due to rigid offsets of the beam will remain coherent and the normalized amplitude of the bunch centroid will remain constant. In contrast, the oscillation due to a deflection that varies from head to tail, such as that due to a transverse wakefields, will damp much like the bunch centroid of a uniform deflection is damped in the BNS damping regime.

Next, we outlined the measurement process where we suggest varying both the charge and the bunch length. In most designs, it is straightforward to increase the bunch length. This can be done in the bunch compressors with minimal impact on the other accelerator components [22]. Changing the beam charge is more problematic since it will affect the upstream performance, which may cause variations in injection into the linac; this needs to be investigated further.

There is an alternate measurement technique using the long-range transverse wakefield [23] that we have not fully investigated. Here, one would use two bunches, and measure the change in trajectory as the separation between the bunches is varied. Since the frequency of the dipole wakefield is roughly 1.5 times that of the accelerating mode, there are substantial variations in the deflecting force when changing rf buckets. Such a technique would likely be easier to implement than varying the bunch charge.

Finally, we have performed initial simulations to verify our technique for the 500-GeV c.o.m. SLAC NLC linear collider design. The results are summarized in table 3 and are encouraging. In addition, we have simulated the correction algorithm with stronger wakefields and found that, in this case, it is even more effective at reducing the emittance dilution. Thus, we conclude the correction technique should provide a method of reducing the emittance dilution due to misaligned accelerating structures, especially when the wakefields are strong, and could prove to be a useful complement to the other structure alignment techniques.

Acknowledgement

We thank F.J. Decker for useful suggestions and ethusiasm and A. Chao for discussion regarding BNS damping.

5. Figures

1. Fig. 1. Normalized action of the beam centroid versus distance in the NLC linac for an injection offset of the centroid $y_0 = 0.1\sigma_y$ (solid), and a single structure (dashes), misaligned by $100\,\mu$m, at the beginning of the linac.

2. Fig. 2. Emittance dilution versus wakefield strength for three cases: no correction (solid), correction varying charge and bunch length (dashes), and correction varying only charge (dots); in the SLAC NLC design, $W' = 7 \times 10^{19}\,\mathrm{V/C/m^3}$.

3. Fig. 3. Emittance dilution versus BPM resolution and misalignment magnitude for four cases: one-to-one correction only (solid), method (d) with $\sigma_{res} = 2.0\,\mu$m (dashes), method (d) with $\sigma_{res} = 1.0\,\mu$m (dots), and method (d) with $\sigma_{res} = 0.5\,\mu$m (dash dot).

6. Tables

Table 1. Parameters of the SLAC 500 GeV c.o.m. NLC design.

Bunch charge	$6.5 \times 10^9 e^+/e^-$
Bunch length	$\sigma_z = 100\,$mm; truncated at $\pm 2\sigma_z$
Initial energy spread	$\sigma_{\Delta E/E} = 1\%$; truncated at $\pm 2\sigma_{\Delta E/E}$
Initial energy	10 GeV
Final energy	250 GeV
Accelerating gradient	37 MeV/m
rf phase	$-6°$
Initial β functions	$\check{\beta} = 2.56\,$m, $\hat{\beta} = 14.8\,$m at 10 GeV
Scaling of β with length	proportional to $\sqrt{E}$
FODO cells, phase advance/cell	90°

Table 2. Quadrupole strength, bunch charge, and length for trajectories.

Method	Trajectory	Quad Strength	Bunch Charge	Bunch Length
	1	1	1	1
(a)	2	1	0.2	1
	3	1	1	2
	4	0.85	1	1
	1	1	1	1
(b)	2	1	0.2	1
	3	1	1	2
	1	1	1	1
(c)	2	1	0.2	1
	3	1	1	2
	4	0.85	1	1
	1	1	0.1	1
(d-1)	2	0.85	0.1	1
	3	1.15	0.1	1
	1	1	1	1
(d-2)	2	1	0.2	1
	3	1	1	2

Table 3. 500 GeV SLAC NLC simulation results.

Method	Quad.	BPM	Acc.	$\Delta\epsilon$ [%]
No Correction	0	0	50 μm	170
(a)	0	0	50 μm	14
(b)	0	0	50 μm	8
1-to-1	50 μm	50 μm	50 μm	1660
(c)	50 μm	50 μm	50 μm	14
(d)	50 μm	50 μm	50 μm	20

7. References

[1] T. O. Raubenheimer, "The Preservation of Low Emittance Flat Beams," *Invited paper presented at the 1993 IEEE Part. Acc. Conf.*, Washington, D.C. (1993).

[2] R. Siemann, "Overview of Linear Collider Designs," *Invited paper presented at the 1993 IEEE Part. Acc. Conf.*, Washington, D.C. (1993).

[3] G. E. Fischer, "Ground Motion: An Introduction for Accelerator Builders," *1992 CERN Accelerator School: Magnetic Measurements and Alignment*, Montreux, Switzerland (1992).

[4] C. Adolphsen, *et. al.*, "Beam-Based Alignment Technique for the SLC Linac," *Proc. of the 1989 IEEE Part. Acc. Conf.*, Chicago, IL. (1989).

[5] T. O. Raubenheimer, "A New Technique of Correcting Emittance Dilutions in Linear Colliders," *Nucl. Instr. Meth.*, **A306**:61-64 (1991).

[6] T. O. Raubenheimer and R. D. Ruth, "A Dispersion-Free Trajectory Correction Technique for Linear Colliders," *Nucl. Instr. Meth.*, **A302**:191-208 (1991).

[7] G. Guignard, "Treatment of Nonlinearities in Achromatic Trajectory Correction for Future Linacs," *Proc. of the 1992 European Part. Acc. Conf.*, Berlin, Germany (1992).

[8] V. Balakin, *Proceedings of the Third Int. Workshop on Linear Colliders*, BINP, Protvino, USSR (1991), p. 302.

[9] C. Adolphsen and T. O. Raubenheimer, "Method to Evaluate Steering and Alignment Algorithms for Controlling Emittance Growth," *Presented at the 1993 IEEE Part. Acc. Conf.*, Washington, D.C. (1993).

[10] T. O. Raubenheimer, "Generation and Acceleration of Low-Emittance Flat Beams for Future Linear Colliders," Ph.D. Thesis, Stanford University, SLAC–387 (1991).

[11] J. T. Seeman, "New Compensation of Transverse Wakefield Effects in a Linac by Displacing Accelerator Structures," *Presented at the 1990 Linear Acc. Conf.*, Albuquerque, NM (1990).

[12] See any text on charged particle optics.

[13] A. W. Chao, B. Richter, and C. Y. Yao, *Nucl. Instr. Meth.*, **178**, 1 (1980).

[14] V. Balakin, A. Novokhatsky, V. Smirnov, *Proceedings of the 12th Int. Conf. on High-Energy Accelerators*, Fermilab, (1983), p. 119.

[15] V. Balakin, *Proceedings of the 1988 Workshop on Linear Colliders*, SLAC–Report–355, (1988), p. 55.

[16] J. T. Seeman and N. Merminga, "Mutual Compensation of Wakefield and Chromatic Effects of Intense Linac Bunches," *Presented at the 1990 Linear Acc. Conf.*, Albuquerque, NM (1990).

[17] It was assumed here that $\delta(z)$ is due to an energy deviation. It is also possible to vary the focusing strength with rf quadrupoles.

[18] A. Chao and T. O. Raubenheimer, work in progress.

[19] The SLAC NLC is a future linear collider being designed at SLAC. Parameters can be found in: "Proc. of 5th Int. Workshop on Next-Generation Linear Colliders," SLAC–Report–436 (1993).

[20] K. Kubo, *et. al.*, "A Simulation Program for Phase Space Dynamics in Future Linear Colliders," work in progress.

[21] K. Bane, private communication.

[22] T. O. Raubenheimer, P. Emma, S. Kheifets, "Chicane and Wiggler Based Bunch Compressors for Future Linear Colliders," *Presented at the 1993 IEEE Part. Acc. Conf.*, Washington, D.C. (1993).

[23] D. Burke, private communcation.

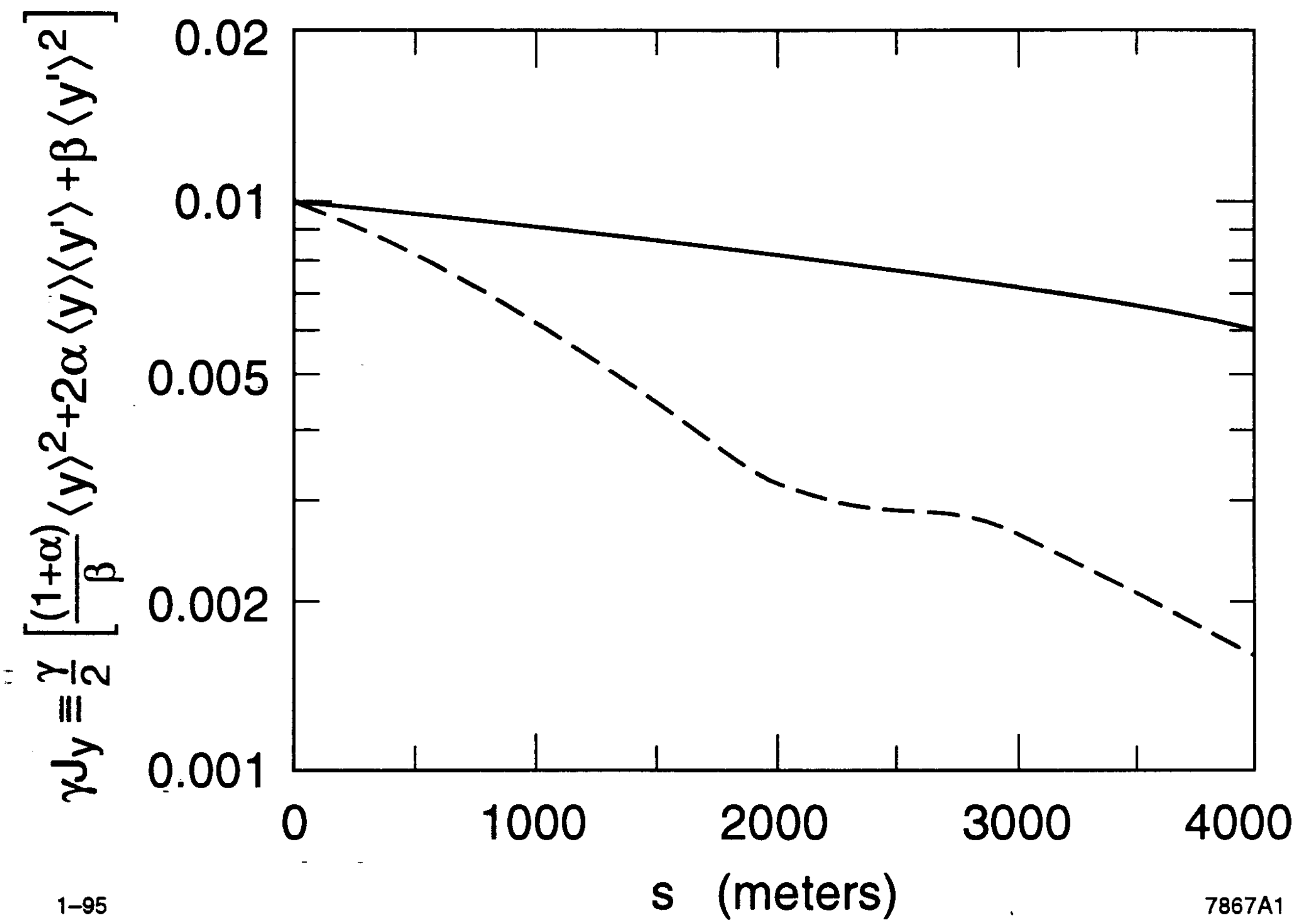

$\gamma J_y \equiv \frac{\gamma}{2}\left[\frac{(1+\alpha)}{\beta}\langle y\rangle^2+2\alpha\langle y\rangle\langle y'\rangle+\beta\langle y'\rangle^2\right]$
0.02
0.01
0.005
0.002
0.001
0
1000
2000
3000
4000
s (meters)
1–95
7867A1

Fig. 1

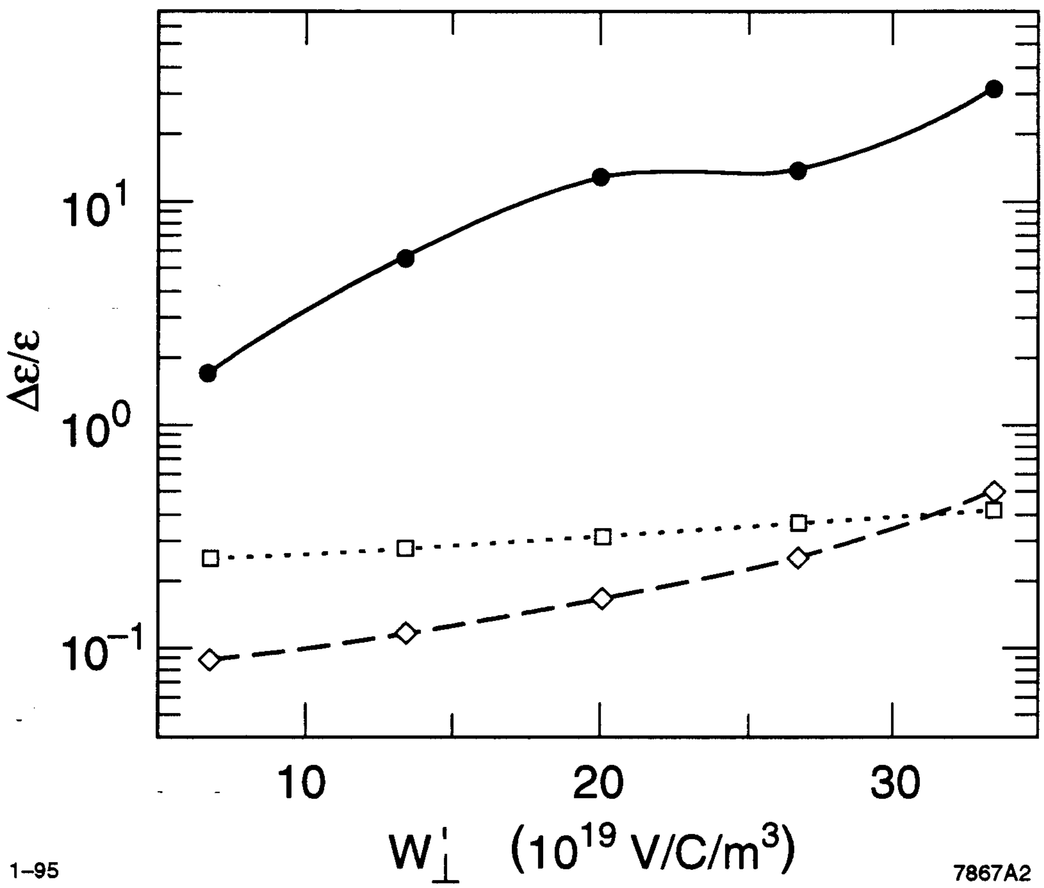

Fig. 2

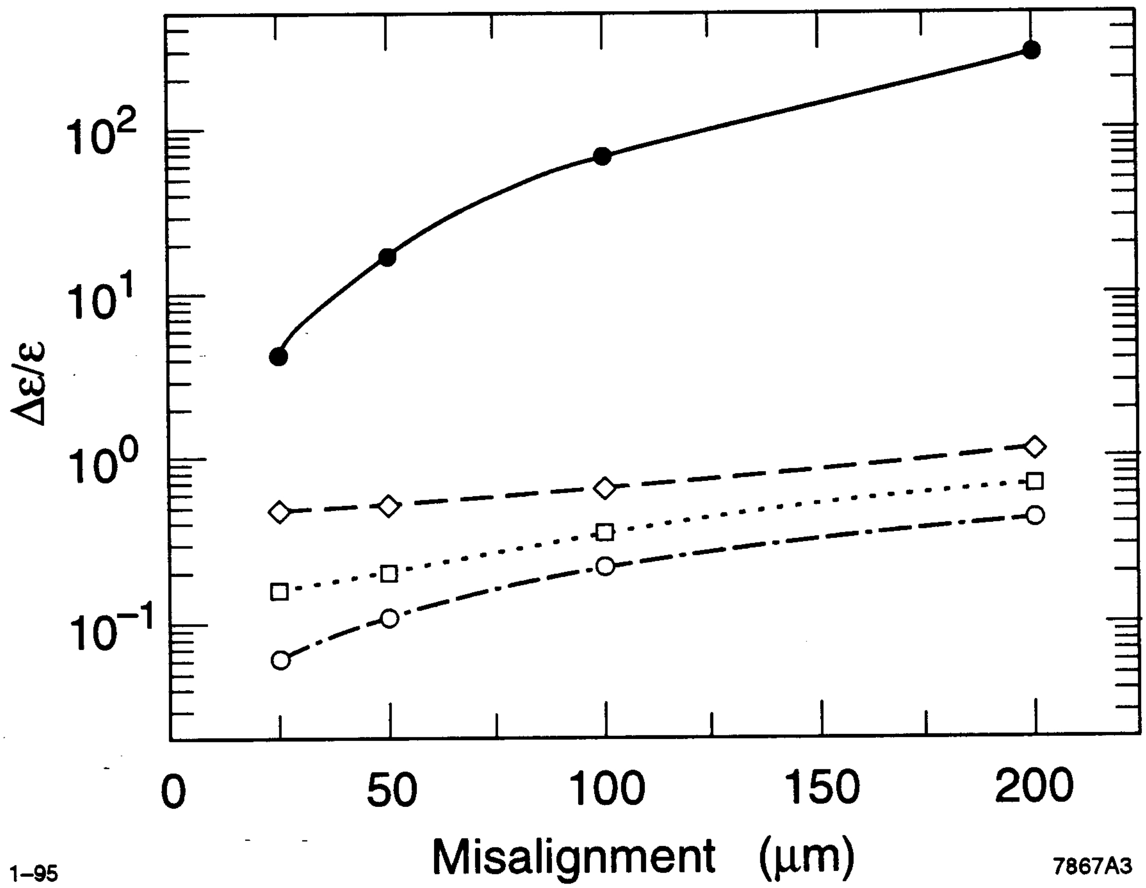

10^2
10^1
10^0
10^{-1}
$\Delta\varepsilon/\varepsilon$
0
50
100
150
200
Misalignment (μm)
1–95
7867A3

Fig. 3